



Geophysical Research Letters

RESEARCH LETTER

10.1029/2020GL088748

Special Section:

The COVID-19 Pandemic:
Linking Health, Society and
Environment

Key Points:

- Seismic noise in a seismographic station within Rio de Janeiro city correlates with mobile-phone isolation indexes
- Seismic noise in Rio de Janeiro can be used as an approximate isolation index
- The best frequency band to capture traffic noise in a large part of the city is 4–8 Hz

Supporting Information:

- Supporting Information S1

Correspondence to:

M. Assumpção,
marcelo.assumpcao@iag.usp.br

Citation:

Dias, F. L., Assumpção, M., Peixoto, P. S., Bianchi, M. B., Collaço, B., & Calhau, J. (2020). Using seismic noise levels to monitor social isolation: An example from Rio de Janeiro, Brazil. *Geophysical Research Letters*, 47, e2020GL088748. <https://doi.org/10.1029/2020GL088748>

Received 5 MAY 2020

Accepted 31 JUL 2020

Using Seismic Noise Levels to Monitor Social Isolation: An Example From Rio de Janeiro, Brazil

Fábio L. Dias¹ , Marcelo Assumpção² , Pedro S. Peixoto³ , Marcelo B. Bianchi² , Bruno Collaço² , and Jackson Calhau²

¹National Observatory, Rio de Janeiro, Brazil, ²Seismology Center, University of São Paulo, São Paulo, Brazil, ³Institute of Mathematics and Statistics, Department of Applied Mathematics, University of São Paulo, São Paulo, Brazil

Abstract Decrease of seismic noise level, after reduction of traffic due to the COVID-19 pandemic, has been observed worldwide. The possibility of using seismic noise as another proxy to estimate social isolation was tested with a station within Rio de Janeiro city. We used the isolation index measured from smartphone movement to calibrate the seismic noise levels and estimated an Isolation Seismic Index, *ISI* (% of the population at home), using the seismic noise energy. Noise levels best correlate with isolation measures in the frequency range 4–8 Hz. Small differences between the smartphone and the *ISI* indexes are interpreted as differences in social activities and noise sources. All mobility indexes are proxies to the actual isolation. Although *ISI* does not measure the number of people outside, it measures the number of noise sources (vehicles, trains, factories, etc.) and can be used as additional information to interpret anomalies in other proxies.

Plain Language Summary A seismic station within Rio de Janeiro city showed a drastic reduction of seismic noise after isolation measures imposed by the state government and city council. We show that the seismic noise level, due mainly to traffic, can be used as another proxy for the social isolation and can help interpret variations in the other indexes of people mobility.

1. Introduction

The continuous ground motion recorded at seismic stations is due to different sources of perturbation (noise sources). At long periods (1 to 50 s) it is mainly produced by atmospheric oscillations and ocean waves, with ocean waves giving energy peaks around 5 and 10 s (e.g., Bormann, 2002; Juretzek & Hadzioannou, 2016; Yang & Ritzwoller, 2008). At high frequencies, above a 1 Hz, it is mainly produced by local perturbations, both natural, such as wind and storms, and anthropogenic, such as vehicles and factories (e.g., Díaz et al., 2020; Poli et al., 2020).

In the last decades, seismic noise has been used for many different purposes. Tomography using seismic noise is now a standard tool to investigate Earth's structure from local to global scale (e.g., Bensen et al., 2008; Ekström, 2013; Li et al., 2016; Shapiro et al., 2005). Polarization analyses of seismic noise can give information about atmospheric disturbances in the oceans (e.g., Schimmel et al., 2011; Stutzmann et al., 2009). High-frequency noise, even within cities, is also extensively used to map soil structure (e.g., Bonnefoy-Claudet et al., 2006; Wathelet et al., 2020). Noise signals have also been identified from other anthropogenic activities such as crowds of people jumping at football matches (Díaz et al., 2017), dancing events (Green & Bowers, 2008), vibrations due to rapid mudflow downstream after a dam rupture (Agurto-Detzel et al., 2016), or long-term changes associated with economic growth (Hong et al., 2020). A good review of noise types recorded in the urban environment, like subway trains and marathons, is given by Díaz et al. (2020).

The most recent observation of variations in human-induced seismic noise is the significant decrease of noise levels due to social isolation policies imposed by governments to reduce the rate of transmission of the COVID-19 pandemic. Several seismological centers around the world have reported through their social media channels (like Facebook and Twitter) the noise reduction especially in stations close to urban centers (Gibney, 2020; Lecocq et al., 2020; Poli et al., 2020). Examples from stations in cities like Milan, Los Angeles, and Barcelona can be found on the National Geographic Magazine website (<https://www.nationalgeographic.com/science/2020/04/coronavirus-is-quieting-the-world-seismic-data-shows/>; last accessed 31 July 2020).

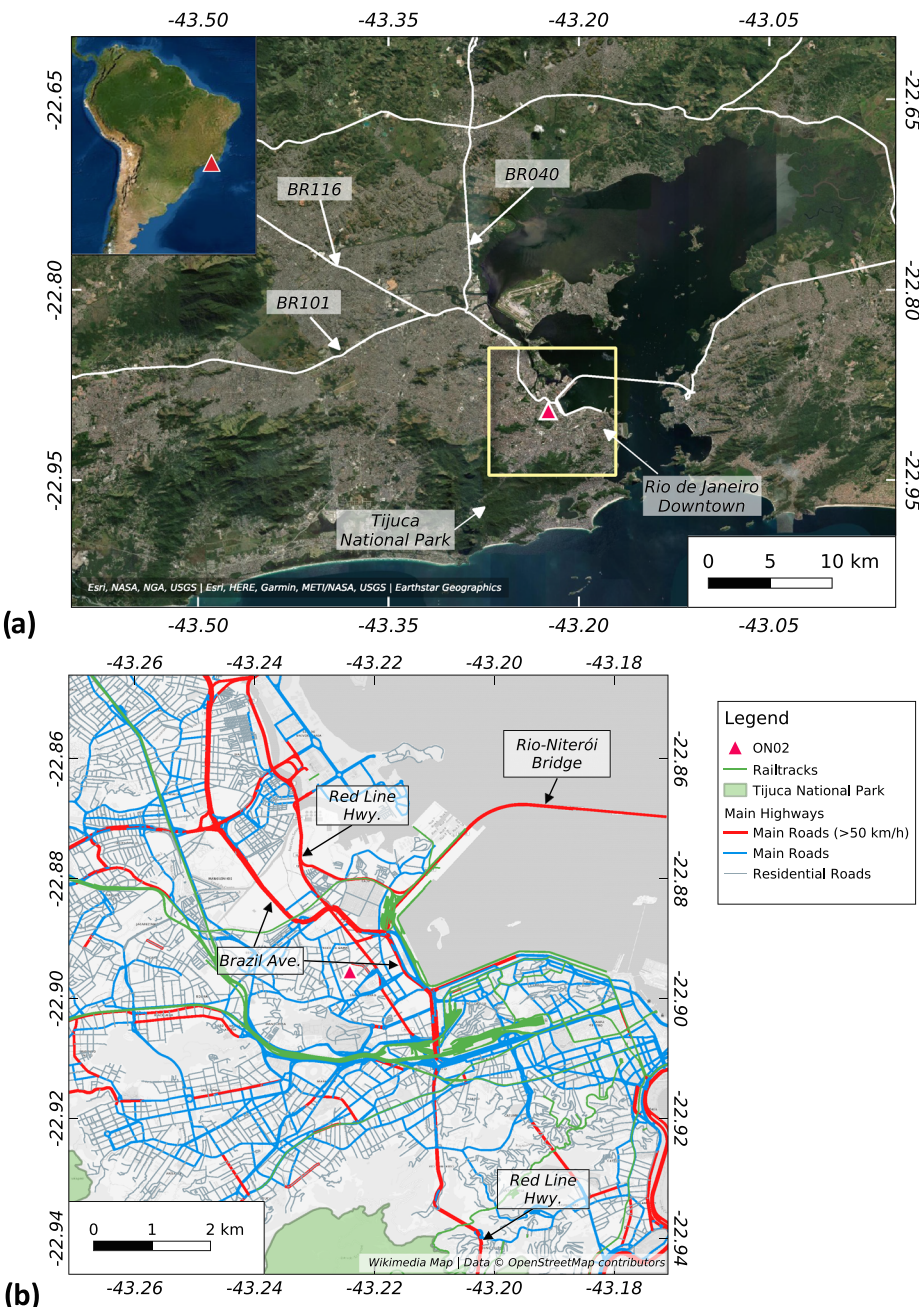


Figure 1. (a) Location of the National Observatory (red triangle) in the Rio de Janeiro metropolitan area, with the seismic station ON.ON02. The station is located ~4 km NW of the busiest city center. White lines are the main access highways (BR040, BR101, and BR116). (b) Street type in Rio de Janeiro: Red lines are highways, blue main avenues, and gray local streets. Green lines are rail tracks. Note N-S running “Brazil Avenue” and “Red Line” just east of the station and fewer busy streets to the west and SW. Green-shaded areas are hills and city parks of Rio de Janeiro. Panel (b) uses data from Wikimedia Maps and OpenStreetMap project available online (<https://maps.wikimedia.org/>). Federal highways in panel (a) are from GeoLogística, Brazil (<https://geo.epl.gov.br/portal/home/>).

2020). In all those examples, it is possible to see the decrease of the ground displacement after mid-March imputed by the beginning of the lockdown in the cities. Another interesting feature is the difference of the noise levels between diurnal and nocturnal period and between weekdays and weekends.

The National Observatory is a research institution located in an urban area in Rio de Janeiro city (Figure 1). The test station, ON02, is installed in the lower floor of an office building on a 3.5-m-tall underground pillar

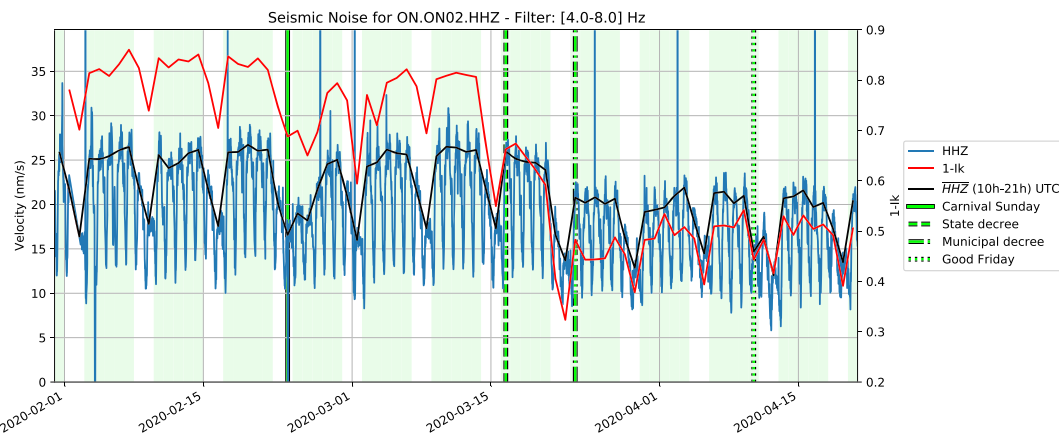


Figure 2. Vertical component particle velocity at ON.ON02 in Rio de Janeiro city (1 February to 20 April 2020). Comparison of seismic noise level (blue and dark blue lines, in nm/s, left scale) with the “In Loco” Social Isolation Index (I_k , red line, fraction of the population staying at home). Note that we plot $(1 - I_k)$, which measures the percentage of people outside. The light blue line is hourly medians of the seismic noise showing higher levels during the day and lower at night. The dark blue curve shows daily median amplitudes (07:00 to 18:00 local time). Background color shows weekdays in green and Saturday and Sundays in white. Dates in the horizontal axis are plotted at the beginning of the day (00:00 local time). Weekends have lower seismic noise both at day and night compared to weekdays. The dashed and dot-dashed green vertical lines are the dates of the social isolation decree by the state government (16 March) and city council (23 March), respectively. Solid and dotted vertical lines are the Sunday Carnival and Good Friday holidays. After the isolation decrees, daytime noise on weekdays reduced from averages of about 26 to 21 nm/s, while the number of people outside decreased from about 80% to less than 50% in the first lockdown week. Plotting script by Thomas Lecocq (Belgian Observatory, <https://github.com/ThomasLecocq>, last accessed 4 May 2020).

that reaches the local rock basement. It is a broadband station (100–50 Hz response) recording at 100 sps. It showed a dramatic decrease in its noise level, especially during the day (Figure 2). Although this effect is better seen at ON02 station, which is inside a city, a few other stations of the Brazilian Seismic Network (Bianchi et al., 2018) closer to median-sized cities (less than 100,000 inhabitants) have also shown a clear decrease in their diurnal noise level. These observations suggest that noise levels could be used to help monitor the compliance with the social isolation policies. Here, we compare the seismic noise reduction with an isolation index, commonly used in Brazil, measured by monitoring the number of smartphones that leave their homes. We show that the seismic noise energy has an excellent correlation with the smartphone-derived isolation index.

2. Origin of the Noise Measured Within Rio de Janeiro City

The noise recorded by seismic stations near or within a city, at frequencies above 1 Hz, is commonly interpreted as due mainly to anthropogenic sources. The significant decrease in noise levels during the COVID-19 lockdown has enabled a clear determination that the “cultural noise” spans the frequency range of 1–40 Hz, but mostly between 2 and 20 Hz (Díaz et al., 2020; Poli et al., 2020). Poli et al. (2020) showed that different cities have different spectra of anthropogenic noise, depending on the type of sources in the vicinity of the station. However, the noise character and type of sources remained the same before or during the lockdown, as shown by the constant average H/V spectral amplitude ratios.

The noise can be produced by a few weak local sources or by many energetic sources at longer distances. We cannot directly determine the dominant distances using a single station. Here we used polarization analysis to infer the possible origins of the noise recorded at ON02. It is usually accepted that most of the high-frequency noise (despite not all) is composed of surface Rayleigh waves (e.g., Bonnefoy-Claudet et al., 2006; Bonnefoy-Claudet, Cornou, et al., 2006). We applied the time-frequency polarization analysis (Schimmel et al., 2011; Schimmel & Gallart, 2003, 2004) to identify the trains of elliptically polarized noise with retrograde particle motion in a vertical plane, for different frequency bands. The distribution of the directions of arrival of such Rayleigh-type noise is shown in Figure 3.

For high frequencies (10–20 Hz) the predominant directions are NE and E, both before and during the quarantine. We interpret this high-frequency noise as coming predominantly from the road traffic of the major highways and avenues close to the station, which run in a N-S direction just east of the National

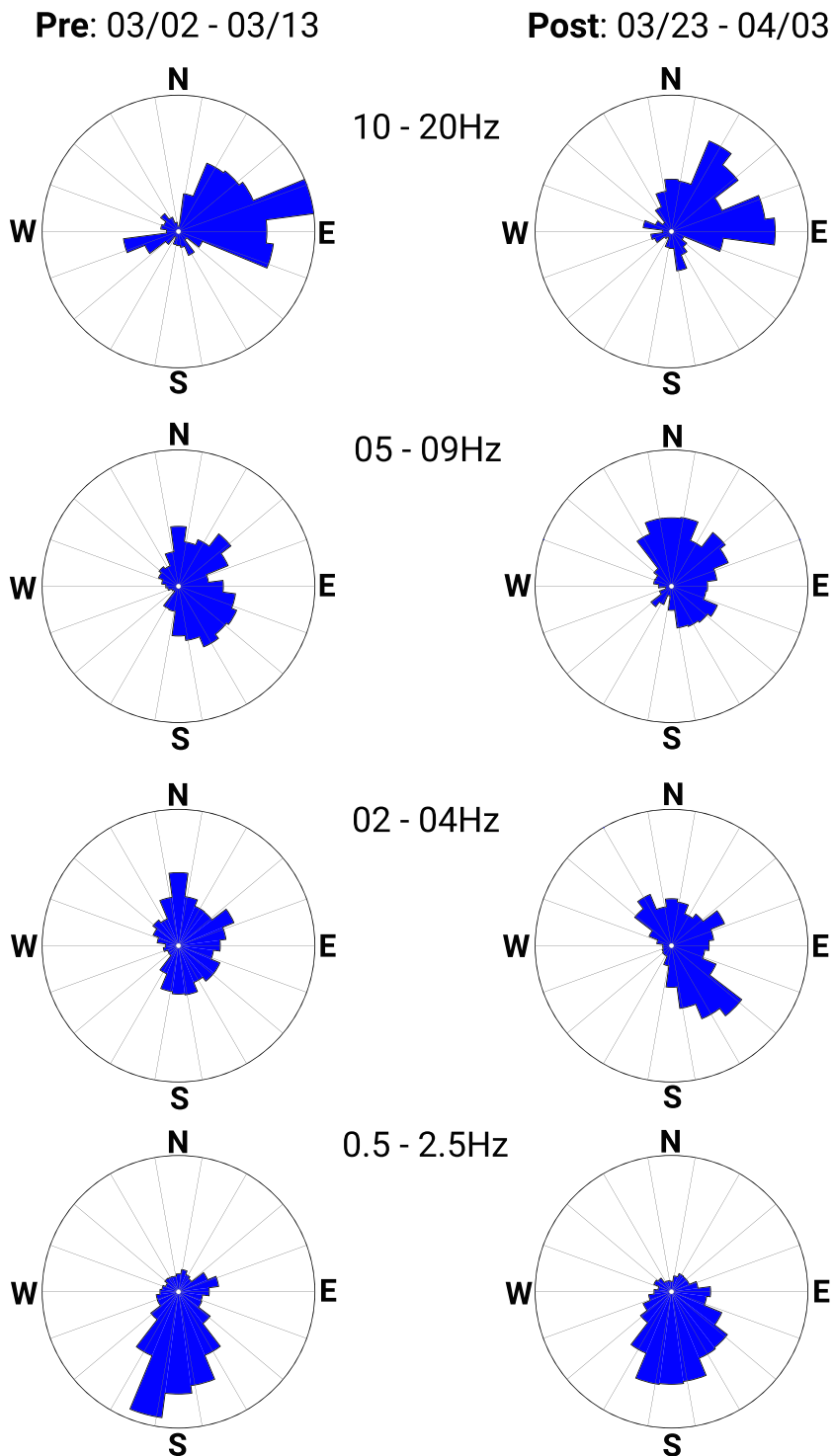


Figure 3. Arrival directions of Rayleigh waves at ON02 for various frequency bands. The left and right columns show directions before and after the isolation decrees, respectively. Processed periods are Monday–Thursday, 07:00 a.m. to 06:00 p.m. local time, for 2 weeks. No consistent difference is observed before or during the quarantine.

Observatory (such as “Brazil Avenue” and “Red Line,” leading to interstate expressways, Figure 1). For intermediate frequencies (2–9 Hz), the incoming directions are more scattered among N, NE, E, SE, and S. Only the W and SW directions have almost no contribution. This probably indicates noise sources from more distant traffic, up to several kilometers maybe (Figure 1b), with the lack of heavy traffic correlating

with the hills and mountains W and SW of the Observatory (green color of national parks, Figure 1). For lower frequencies, around 1 Hz, the dominant sources are to the south, which is interpreted as influence of the more distant oceanic microseisms.

No clear systematic difference was observed in the predominant directions before and during the quarantine. This is consistent with the findings of Poli et al. (2020) for stations in northern Italy where the noise character remains the same before and during the quarantine, only its amplitude changes.

Although this polarization analysis is qualitative, it shows that a 2–9 Hz frequency band is convenient to sample traffic noise in a large area of the city. Significant contribution from local activity of the Observatory itself, below 20 Hz, can be discarded. The Observatory lies in a residential area, without operation of heavy equipment in the institution where only technical and research staff work. Working hours start at 09:00 a.m., but the average noise in the range 4–14 Hz reaches its daily average about 05:30 a.m. local time (see supporting information Figure S1), due to traffic in the neighborhood and the city in general. This discards a significant contribution from local activities of the Observatory.

3. The Social Isolation Index (I_k) and the Isolation Seismic Index (ISI)

We use the smartphone isolation index to calibrate the noise level as a proxy for the number of noise sources in the city. We assume that the smartphone movement away from home is directly proportional to the number of seismic sources (mainly cars, trains, buses, and factories) operating during the day.

3.1. The Smartphone Index I_k

The Brazilian company *In Loco* (www.inloco.com.br) collects the positions of more than 37 million smartphones, all over Brazil, when they are using their *SDK* (*software development kit*), which is present in many popular mobile apps. No personal information is gathered. The anonymized data collected by *In Loco* contain the physical locations where billions of visits to selected apps have occurred. The technology uses not only Global Positioning System (GPS) data but also wireless and other mobile sensors that combined allow a precision of meters for the locations. Based on the pattern of similar positions outside working hours, it is possible to define their home or neighborhood location and then measure the number of times each smartphone moves more than a few hundreds of meters away from home or their neighborhood, for more than 5 min, within 24 hr. A more detailed explanation of their methodology can be found in Peixoto et al. (2020). The *In Loco* isolation index is provided by the company already in aggregated form, by cities, therefore totally preserving anonymity, since no individual data were available for this research. The index measures the fraction of people that stay at home and is defined as

$$I_k = \frac{n_k^{\text{res}} - n_k^{\text{mov}}}{n_k^{\text{res}}}$$

where n_k^{res} is the estimated total number of city residents in the *In Loco* database and n_k^{mov} is the number of smartphones used outside their home location in day k . Before the lockdown decree, on 23 March, I_k was about 0.2 on average (Figure 2), indicating that about 80% of people used to be away from home. For Rio de Janeiro city, the *In Loco* system captures ~10% of the population (mainly the more economically active individuals). The database is not a census of all individuals' locations, but it has been shown to capture well the overall population mobility (Candido et al., 2020; Peixoto et al., 2020).

3.2. The Isolation Seismic Index (ISI)

According to the definition, the fraction of people out of home is given by $(1 - I_k)$. We assume that the number of noise sources (vehicles, trains, trucks, and working factories) is proportional to $(1 - I_k)$ and they are the main sources that contribute to the records at the station. That is, for a high-noise station within a city, natural sources of noise (wind, rain, etc.) are usually insignificant. We also assume that the energy of the seismic waves, for a frequency range of 2–20 Hz (dominated by anthropogenic noise), is proportional to the square of the particle velocity. Therefore, we expect that $(1 - I_k)$ should be proportional to the noise "energy."

We measure the noise levels as follows: (a) remove the instrument response and calculate the power spectral density for the particle velocity for every 15 min segment with overlap of 7.5 min; (b) integrate the velocity

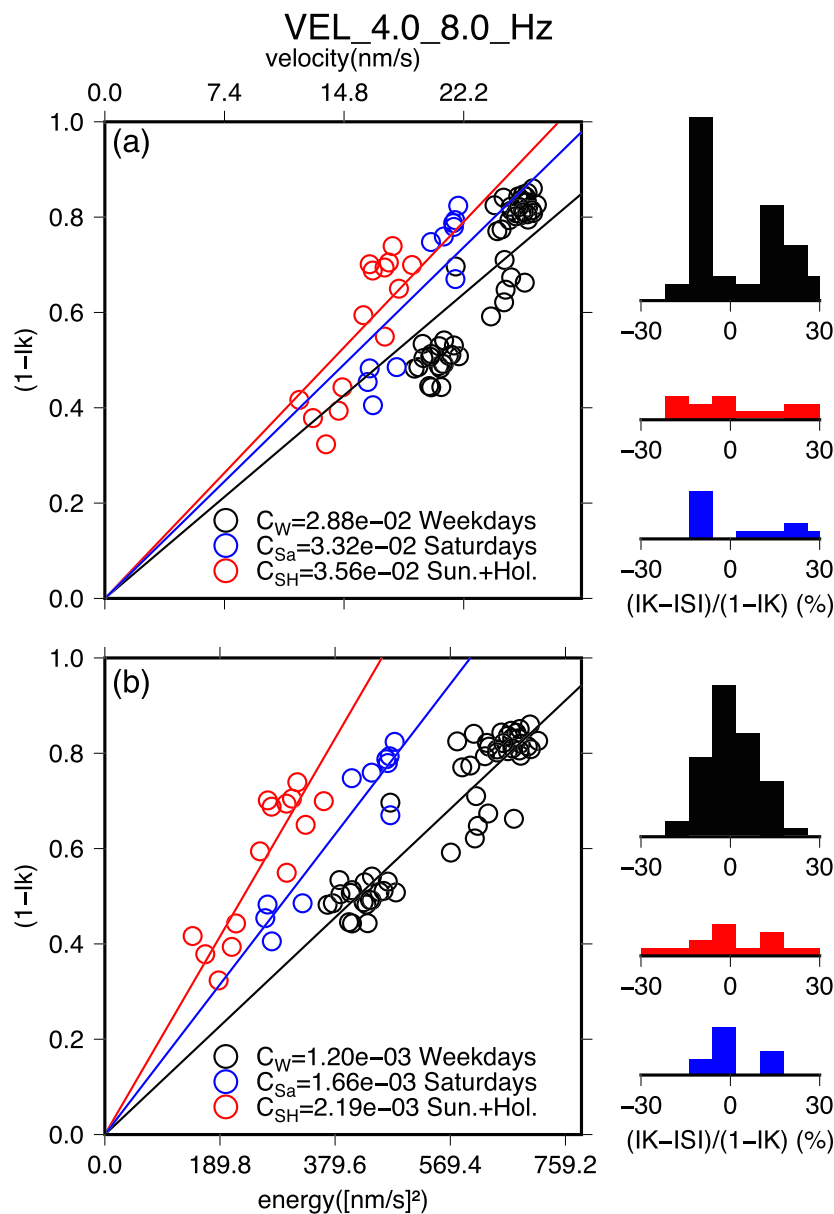


Figure 4. Relation between the average diurnal noise (07–18 hr local time) and the fraction of people outside ($1 - I_k$). (a) Average amplitude and (b) average “energy” (velocity squared). I_k is the *In Loco* isolation index (fraction of people staying at home); therefore, $(1 - I_k)$ is fraction of people outside. Black circles are weekdays, red are Sundays and holidays, and blue are Saturdays or bridges. Note the clear linear relation between energy and $(1 - I_k)$. During weekdays the number of heavy noise sources (trucks, trains, and working factories) is relatively higher than on Sundays and holidays, for the same number of people outside. Saturday plots at midway between weekdays and Sundays. The histograms show the relative errors (in percentage) of the seismic “outside index” $(1 - ISI)$ in relation to the smartphone index. Smaller errors are seen for the energy (bottom histograms) compared with the amplitude (top).

power spectral density, in a certain frequency band, to estimate the *rms* particle velocity for each segment; and (c) get the *rms* median value of for all segments between 07:00 a.m. and 06:00 p.m. local time. Taking medians, instead of the averages, avoids the influence of spurious bursts of noise from very local disturbances. These calculations were done with a script based on a code by Thomas LeCocq (<https://github.com/ThomasLecocq/SeismoRMS>—last accessed May 2020).

We tested various frequency ranges and found that 4–8 Hz best correlates with the mobile-phone isolation index (Figure S2). This is consistent with our comparison of the polarization results with the expected

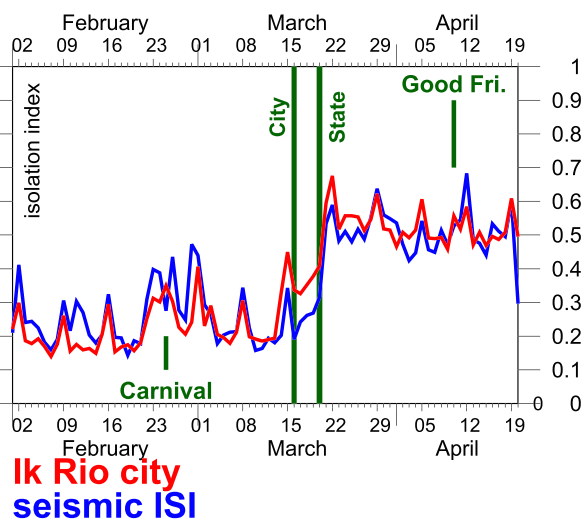


Figure 5. Comparison of the Social Isolation Index (red line for the city of Rio de Janeiro) with the Isolation Seismic Index, *ISI* (blue line). The days annotated in the horizontal axis are Sundays. The vertical short green lines show the Carnival (Tuesday, 25 February) and the Good Friday (10 April) holidays. The two vertical green lines indicate the dates of the state and city council isolation decrees.

traffic: Noise from this frequency range probably comes from more distant sources in the city and are, therefore, more representative of the whole city where the isolation index I_k was obtained.

Figure 4 compares the fraction of people staying out of their homes, $(1 - I_k)$, with both the median amplitude and energy (i.e., median amplitude squared) of the diurnal particle velocity (between 10 and 21 hr UTC, 07–18 hr local time), for the best fitting band 4–8 Hz. It is clear, from the histogram shapes and reduced errors in the fit (Figure S2), that the square of the amplitudes has a better linear relation with the $(1 - I_k)$ index, compared with the amplitude, as expected. Therefore, we can estimate a calibration constant with

$$(1 - I_k) = C (A_k)^2 \quad (1)$$

Figure 4 also shows that the relation between I_k and noise is different between weekdays, Saturdays, and Sundays + holidays. One possible interpretation is that on Sundays and holidays, people leave home mainly using light vehicles; heavier sources of noise (trucks, trains, buses, working factories, etc.) are mainly operated on weekdays. Saturday is halfway between Sunday and workdays where factories and commerce are partially functioning.

The good correlation between I_k and noise energy allows us to define an “Isolation Seismic Index”, *ISI*, as

$$(1 - ISI_k) = C (A_k)^2 \quad (2)$$

where coefficient C can have three values: $C = C_W$ for working weekdays, C_{Sa} for Saturdays, and $C = C_{SH}$ for Sundays and holidays. Based on Figure 4, we obtained $C_W = 0.00120$, $C_{Sa} = 0.00166$, and $C_{SH} = 0.00219$. One interpretation of the C values is that for the same noise amplitude, we must expect less isolation (i.e., higher $1 - I_k$) on the weekend than on the weekdays.

In Figure 4, we also show the histograms of the difference (in percentage) between the measured index $(1 - I_k)$ by the In Loco company and the *ISI* value predicted by the coefficient C using the amplitude and energy of the signal. The histograms for the energy, in all situations, are more concentrated around zero than histograms for the amplitude, reinforcing the better agreement of the energy and isolation index. Another conclusion is that the difference between I_k and *ISI* is concentrated within $\pm 20\%$. The *rms* fit, in percentage, in Figure 4b, is 11%. For example, if the noise level indicates a seismic isolation index of 0.40 (i.e., 40% isolated and 60% outside), the expected uncertainty would be 6.6% (11% of 0.60).

Figure 5 shows the Isolation Seismic Index for Rio de Janeiro city (blue line) compared to the *In Loco* smartphone isolation index I_k . The *ISI* level on the weekdays after the lockdown decree matches the smartphone-derived index quite well, as well as the variation between weekends and weekdays.

4. Discussion

A detailed comparison between *ISI* and I_k indexes (Figure 5) shows that, despite the overall excellent agreement (using only two parameters, C_W and C_{SH} ; for Saturday, we used the average between C_W and C_{SH}), small inconsistencies are observed, which can help in interpretation of social isolation and mobility patterns.

In the week of 16 to 20 March (Monday to Friday), the seismic index continues in the same level as the previous working weeks, whereas the I_k index shows that many people had already started to stay at home. One possible interpretation is that, before the city council decree imposing severe isolation after 22 March (closing all shops, restaurants, commerce, etc.), many people had already started reducing their social activities due to the previous state decree of 16 March, prohibiting large gatherings and closing cinemas, theater,

sports, schools, and even interstate bus trips. These early isolation steps, however, may not have affected industries, commerce, services, and municipal public transportation, which maintained the number of heavy seismic noise sources in the same level, until the definite lockdown on 23 March, Monday.

5. Conclusions

The government quarantine, due to the COVID-19 pandemic, drastically reduced the mobility of the population and commercial activity. Owing to those restrictions the noise level recorded at seismographic stations close to urban centers decreased significantly. Here, we show this effect at station ON02 situated at an urban area of Rio de Janeiro city. We compared the average particle velocity recorded by that station with the Social Isolation Index (I_k), measured through smartphone location monitoring, and showed that both are closely related: The noise level decreases as the Social Isolation Index increases. The correlation is good enough to allow an “Isolation Seismic Index” to be defined, after calibration with the smartphone-derived index.

The Isolation Seismic Index does not measure directly the number of people outside but estimates the number of active noise sources such as trains, buses, vehicles, and factories and so can be used as additional information to interpret anomalies in the other proxies.

Data Availability Statement

Figure 2 was made using Thomas Lecocq code <https://github.com/ThomasLecocq/SeismoRMS> (last accessed 4 May 2020). Data for the Rio de Janeiro station ON.ON02 are available at the database of the Brazilian Seismographic Network (www.rsrbr.gov.br). In Loco isolation indexes can be viewed at their site (www.inloco.com.br). The data used here (daily noise median amplitudes and I_k indexes are available at a Zenode repository (<https://doi.org/10.5281/zenodo.3944747>).

Acknowledgments

We thank company In Loco for their raw isolation indexes. F. L. D. benefited from Petrobras Grant 2017/00159-0 and M. A. from the Brazilian National Research Council (Conselho Nacional de Desenvolvimento Científico e Tecnológico; Grant 301284/2017-2). P. S. P. acknowledges the São Paulo State Research Foundation (Fundação de Amparo à Pesquisa do Estado de São Paulo [FAPESP]) Grant 16/18445-7.

References

- Agurto-Detzel, H., Bianchi, M., Assumpção, M., Schimmel, M., Collaço, B., Ciardelli, C., et al. (2016). The tailings dam failure of 5 November 2015 in SE Brazil and its preceding seismic sequence. *Geophysical Research Letters*, 43, 4929–4936. <https://doi.org/10.1002/2016GL069257>
- Bensen, G. D., Ritzwoller, M. H., & Shapiro, N. M. (2008). Broad-band ambient noise surface wave tomography across the United States. *Journal of Geophysical Research*, 113, B05306. <https://doi.org/10.1029/2007JB005248>
- Bianchi, M. B., Assumpção, M., Rocha, M. P., Carvalho, J. M., Azevedo, P. A., Fontes, S. L., et al. (2018). The Brazilian Seismographic Network (RSBR): Improving seismic monitoring in Brazil. *Seismological Research Letters*, 89(2A), 452–457. <https://doi.org/10.1785/0220170227>
- Bonnefoy-Claudet, S., Cornou, C., Bard, P.-Y., Cotton, F., Moczo, P., Kristek, J., & Donat, F. (2006). H/V ratio: A tool for site effects evaluation. Results from 1-D noise simulations. *Geophysical Journal International*, 167(2), 827–837. <https://doi.org/10.1111/j.1365-246X.2006.03154.x>
- Bonnefoy-Claudet, S., Cotton, F., & Bard, P. Y. (2006). The nature of noise wavefield and its applications for site effects studies: A literature review. *Earth-Science Reviews*, 79(3–4), 205–227. <https://doi.org/10.1016/j.earscirev.2006.07.004>
- Bormann, P. (2002). Seismic signals and noise. In P. Bormann (Ed.), *IASPEI new manual of seismological observatory practice* (Chap. 4, Vol. 1, pp. 1–33). Potsdam, Germany: GeoForschungsZentrum.
- Candido, D., Claro, I. M., de Jesus, J. G., de Souza, W. M., Moreira, F. R. R., Dellicour, S., et al. (2020). Evolution and epidemic spread of SARS-CoV-2 in Brazil. *Science*. <https://doi.org/10.1101/2020.06.11.20128249v2>
- Díaz, J., Ruiz, M., Sánchez-Pastor, P. S., & Romero, P. (2017). Urban seismology: On the origin of earth vibrations within a city. *Scientific Reports*, 7, 15296. <https://doi.org/10.1038/s41598-017-15499-y>
- Díaz, J., Schimmel, M., Ruiz, M., & Carbonell, R. (2020). Seismometers within cities: A tool to connect Earth Sciences and Society. *Frontiers in Earth Science*, 8(9). <https://doi.org/10.3389/feart.2020.00009>
- Ekström, G. (2013). Love and Rayleigh phase-velocity maps, 5–40 s, of the western and central USA from USArray data. *Earth and Planetary Science Letters*, 402, 42–49. <https://doi.org/10.1016/j.epsl.2013.11.022>
- Gibney, E. (2020). Coronavirus lockdowns have changed the way Earth moves. *Nature*, 580, 176–177 (2020–March 31). <https://doi.org/10.1038/d41586-020-00965-x>
- Green, D. N., & Bowers, D. (2008). Seismic raves: Tremor observations from an electronic dance music festival. *Seismological Research Letters*, 79(4), 546–553. <https://doi.org/10.1785/gssrl.79.4.546>
- Hong, T. K., Lee, J., Lee, G., Lee, J., & Park, S. (2020). Correlation between ambient seismic noises and economic growth. *Seismological Research Letters*, 91, 2343–2354. <https://doi.org/10.1785/0220190369>
- Juretzek, C., & Hadzioannou, C. (2016). Where do ocean microseisms come from? A study of Love-to-Rayleigh wave ratios. *Journal of Geophysical Research: Solid Earth*, 121, 6741–6756. <https://doi.org/10.1002/2016JB013017>
- Lecocq, T., Hicks, S. P., van Noten, K., van Wijk, K., Koolemeijer, P., de Plaen, R. S. M., et al. (2020). Global quieting of high-frequency seismic noise due to COVID-19 pandemic lockdown measures. *Science*, eabd2438. <https://doi.org/10.1126/science.abd2438>
- Li, C., Yao, H., Fang, H., Huang, X., Wan, K., Zhang, H., & Wang, K. (2016). 3D near-surface shear-wave velocity structure from ambient-noise tomography and borehole data in the Hefei urban area, China. *Seismological Research Letters*, 87(4), 882–892. <https://doi.org/10.1785/0220150257>
- Peixoto, P. S., Marcondes, D., Peixoto, C., & Oliva, S. M. (2020). Modeling future spread of infections via mobile geolocation data and population dynamics. An application to COVID-19 in Brazil. *PLOS ONE*, 15(7). <https://doi.org/10.1371/journal.pone.0235732>

- Poli, P., Boaga, J., Molinari, I., Cascone, V., Boschi, L. (2020). The 2020 coronavirus lockdown and seismic monitoring of anthropic activities in Northern Italy. *Scientific Reports*, 10(9404). <https://doi.org/10.1038/s41598-020-66368-0>
- Schimmel, M., & Gallart, J. (2003). The use of instantaneous polarization attributes for seismic signal detection and image enhancement. *Geophysical Journal International*, 155(2), 653–668. <https://doi.org/10.1046/j.1365-246X.2003.02077.x>
- Schimmel, M., & Gallart, J. (2004). Degree of polarization filter for frequency dependent signal enhancement through noise suppression. *Bulletin of the Seismological Society of America*, 94(3), 1016–1035. <https://doi.org/10.1785/0120030178>
- Schimmel, M., Stutzmann, E., Arduhin, F., & Gallart, J. (2011). Polarized Earth's ambient microseismic noise. *Geochemistry, Geophysics, Geosystems*, 12, Q07014. <https://doi.org/10.1029/2011GC003661>
- Shapiro, N. M., Campillo, M., Stehly, L., & Ritzwoller, M. H. (2005). High-resolution surface-wave tomography from ambient seismic noise. *Science*, 307(5715), 1615–1618. <https://doi.org/10.1126/science.1108339>
- Stutzmann, E., Schimmel, M., Patau, G., & Maggi, A. (2009). Global climate imprint on seismic noise. *Geochemistry, Geophysics, Geosystems*, 10, Q11004. <https://doi.org/10.1029/2009GC002619>
- Wathelet, M., Chatelain, J. L., Cornou, C., Giulio, G. D., Guillier, B., Ohrnberger, M., & Savvaidis, A. (2020). Geopsy: A user-friendly open-source tool set for ambient vibration processing. *Seismological Research Letters*, XX, 91, 1878–1889. <https://doi.org/10.1785/0220190360>
- Yang, Y., & Ritzwoller, M. H. (2008). Characteristics of ambient seismic noise as a source for surface wave tomography. *Geochemistry, Geophysics, Geosystems*, 9, Q02008. <https://doi.org/10.1029/2007GC001814>